



HAL
open science

Forming morphing microfoam

Spiros Kotopoulos, Michiel Postema

► **To cite this version:**

Spiros Kotopoulos, Michiel Postema. Forming morphing microfoam. 20th International Congress on Acoustics, ICA 2010, Aug 2010, Sydney, Australia. pp.25. hal-03195561

HAL Id: hal-03195561

<https://hal.science/hal-03195561>

Submitted on 11 Apr 2021

HAL is a multi-disciplinary open access archive for the deposit and dissemination of scientific research documents, whether they are published or not. The documents may come from teaching and research institutions in France or abroad, or from public or private research centers.

L'archive ouverte pluridisciplinaire **HAL**, est destinée au dépôt et à la diffusion de documents scientifiques de niveau recherche, publiés ou non, émanant des établissements d'enseignement et de recherche français ou étrangers, des laboratoires publics ou privés.

Forming morphing microfoam

Spiros Kotopoulos (1,2) and Michiel Postema (1,2)

(1) Emmy-Noether Group, Institute of Medical Engineering, Dept. of Electrical Engineering and Information Sciences, Ruhr-Universität Bochum, 44780 Bochum, Germany

(2) Department of Engineering, The University of Hull, Kingston upon Hull HU6 7RX, United Kingdom

PACS: 43.25.Yw; 43.35.Ei.

ABSTRACT

The ultrasound-induced formation of bubble clusters may be of interest as a therapeutic means. If the clusters behave as one entity, *i.e.*, one mega-bubble, its ultrasonic manipulation towards a boundary is straightforward and quick. If the clusters can be forced to accumulate to a microfoam, entire vessels might be blocked on purpose using an ultrasound contrast agent and a sound source. Alternatively, the microfoam could be removed from the blood pool. The latter technique might be applicable in highly toxic ultrasound-guided drug delivery. We analysed how ultrasound contrast agents with different shell compositions form clusters in a capillary and what happens to the clusters if sonication is continued, using continuous driving frequencies in the range 1–10 MHz. We observed the following stages of microfoam formation within a dense population of microbubbles before ultrasound arrival. After the sonication started, contrast microbubbles collided, forming small clusters, owing to secondary radiation forces. These clusters coalesced within the space of a quarter of the ultrasonic wavelength, owing to primary radiation forces. The resulting microfoams translated in the direction of the ultrasound field, hitting the capillary wall, also owing to primary radiation forces.

We have demonstrated that as soon as the bubble clusters are formed and as long as they are in the sound field, they behave as one entity. At our acoustic settings, it takes seconds to force the bubble clusters to positions approximately a quarter wavelength apart. The clusters contain approximately 2,000 ultrasound contrast agent microbubbles. Clusters streaming through a capillary interact, forming morphing microfoam. Subjecting an ultrasound contrast agent of given concentration to a continuous low-amplitude signal makes it cluster to a microfoam of known position and known size, allowing for sonic manipulation, including the release of its contents.

INTRODUCTION

Ultrasound contrast agents are used in diagnostic imaging. They consist of microscopically small bubbles containing slowly diffusing gas encapsulated by biodegradable shells. When inserted in the blood stream, these bubbles oscillate upon ultrasonic sonication, thereby creating detectable ultrasound themselves. A brief overview of the most common ultrasound contrast agents has been presented by Postema and Schmitz (2006). It follows that albumin and lipids are currently the most common bubble encapsulation materials. Because of the proven feasibility to attach therapeutic compounds to albumin and lipids, therapeutic applications of contrast agents have become of interest, as shown by Kudo et al. (2002), Lindner and Kaul (2001), Unger et al. (2002), and Postema and Gilja (2007). It is desirable that the therapeutic load of any such contrast agent is released close to the vessel wall. Therefore, pushing bubbles towards boundaries by means of primary radiation forces has been studied by Dayton et al. (2002) and Tortoli et al. (2005). Both primary and secondary radiation forces resulting from oscillating bubbles, may cause the repulsion or mutual attraction, and eventual collision and coalescence, of contrast agent bubbles. This phenomenon has been less studied.

From the therapeutic point of view, the formation of bubble clusters may be of interest. If the clusters behave as one entity, *i.e.*, one mega-bubble, its ultrasonic manipulation towards a boundary is fairly straightforward and quick. If the clusters can be forced to accumulate to a microfoam, entire vessels might be blocked on purpose using an ultrasound contrast agent and a sound source. Alternatively, the microfoam could be forced

to accumulate for later removal. The latter technique might be applicable in highly toxic ultrasound-guided drug delivery, where bubbles that have been unsuccessful in delivering their contents should be removed from the blood pool.

Kotopoulos and Postema (2010) analysed how ultrasound contrast agent clusters are formed and what happens to the clusters if sonication is continued, showing high-speed camera footage of microbubble clustering phenomena.

THEORY

A brief overview of theory on radiation forces and ultrasound contrast agent has been given in Postema et al. (2007). Bubble translation in the direction of the sound field is caused by a primary radiation force resulting from a pressure gradient across the bubble surface. Secondary radiation forces, resulting from oscillating bubbles under sonication, may cause the mutual attraction and subsequent coalescence of contrast microbubbles. Two bubbles that oscillate in phase approach each other, whereas two bubbles that oscillate out of phase recede from each other, as demonstrated by Leighton (1994) and Postema and Schmitz (2007).

In a standing wave field, bubbles with resonance frequencies higher than the transmitted sound field aggregate at the pressure antinodes, whereas bubbles with resonance frequencies lower than the transmitted sound field aggregate at the pressure nodes, shown by Leighton (1994). Hence, the ultimate distance between clusters must be a quarter of the wavelength.

Both processes of bubble clusters aggregating and the movement of clusters in the direction of the sound field can be approximated by:

$$\frac{dh}{dt} \approx \frac{p_a^2}{6\rho c f \eta} \frac{\delta \left(\frac{f_c}{f}\right)}{\left[\left(\frac{f_c}{f}\right)^2 - 1\right]^2 + \left[\delta \left(\frac{f_c}{f}\right)\right]^2}, \quad (1)$$

where h is the distance travelled by the cluster, p_a is the peak rarefactional acoustic pressure, ρ is the liquid density, c is the speed of sound, η is the shear (dynamic) viscosity of the fluid, δ is the dimensionless total damping coefficient as given by Medwin (1977), f is the driving frequency, and f_c is the cluster resonance frequency, which must be lower than an individual bubble's resonance frequency.

MATERIALS AND METHODS

A schematic overview of our experimental setup for simultaneous optical observations during sonication is shown in Figure 1. A polycarbonate container was built with internal dimensions: $24 \times 18 \times 15$ (cm)³. To give access to a microscope objective lens, a hole with an 11-mm diameter had been drilled in the base, covered with a 2-mm thick test slide (Jencons (Scientific) Ltd, Leighton Buzzard, Bedfordshire, UK). The container was filled with 2.6 L tap water. The container was placed on an $x - y$ -table on top of a DM IRM inverted microscope (Leica Microsystems Wetzlar GmbH, Wetzlar, Germany) with two objective lenses: a 506075 C-Plan 10 \times objective lens (Leica Microsystems Wetzlar GmbH) with a 0.22 numerical aperture and a 506236 N-Plan 50 \times objective lens (Leica Microsystems Wetzlar GmbH) with a 0.50 numerical aperture. A Mille Luce™ Fiber Optic Illuminator Model M1000 (StockerYale, Inc., Salem, NH, USA) was connected to an optic fibre with a 7-mm diameter leading into the water of the container. It was placed in line with the objective lens, as shown in Figure 2.

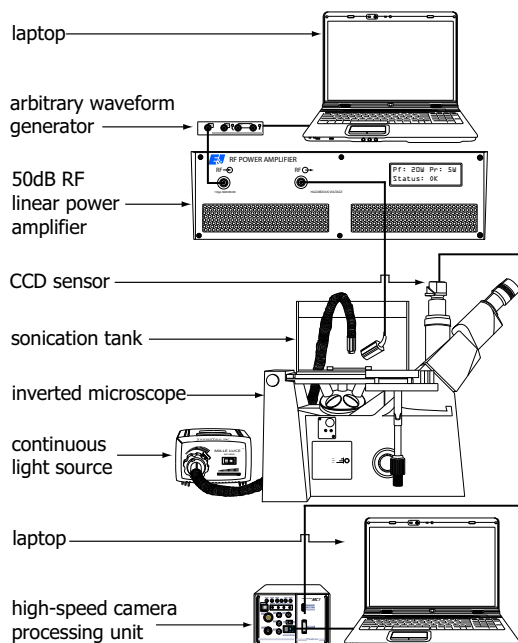


Figure 1: Schematic overview of the experimental setup.

The charge couple device (CCD) of a FASTCAM MC1 high-speed camera (Photron (Europe) Limited, West Wycombe, Bucks, United Kingdom) was mounted to the microscope and connected to its processing unit, which was capable of record-

ing images at 10,000 frames per second. The camera was controlled by a laptop computer.

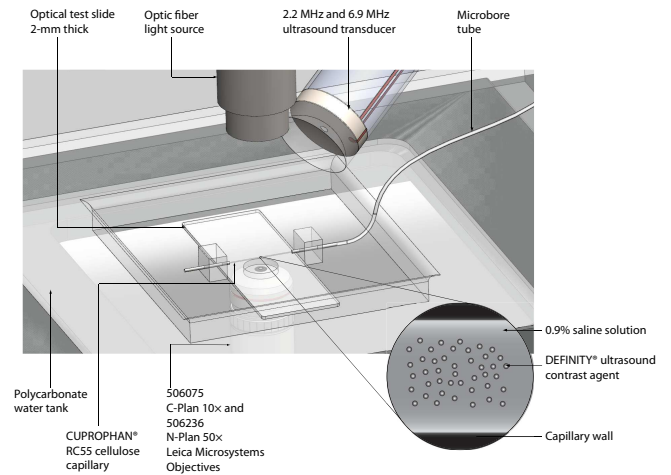


Figure 2: Close-up of the sonication tank with coinciding sound, light beam, and objective focus.

Ultrasound

A laptop computer triggered a DATAMAN-530 arbitrary waveform generator (Dataman Programmers Ltd, Maiden Newton, Dorset, UK), which was connected to a 2100L 50-dB RF power amplifier (Electronics & Innovation Ltd., Rochester, NY, USA). The power amplifier was connected to an undamped broadband single element transducer containing a Pz37 Piezo crystal (Ferroperm Piezoceramics A/S, Kvistgård, Denmark) with a centre frequency of 2.2 MHz. The design of the transducer has been described by Kotopoulos et al. (2009). Transmitted signals were typically continuous with frequencies in the range 1–10 MHz. The peak-negative acoustic pressures were determined using a PVdF needle hydrophone system with a 0.2-mm probe (Precision Acoustics Ltd, Dorchester, Dorset, UK) connected to a TDS 420A oscilloscope (Tektronix, Inc., Beaverton, OR, USA).

The ultrasound transducer was positioned in the container using a clamp stand, at a focal distance of 38 mm from the region of interest to be studied. The azimuth of the length axis of the transducer relative to the North of the container was 37° and the elevation of the length axis of the transducer relative to the base of the container was 17°.

Ultrasound contrast agent

DEFINITY® (Lantheus Medical Imaging, North Billerica, MA, USA) consists of C₃F₈ gas microbubbles with mean diameters between 1.1 and 3.3 μm, encapsulated by lipid/surfactant shells. Kimmel et al. (2007) measured its resonance frequency to be 2.7 MHz. The 1.5-ml vials used in our experiments had been stored at 9°C. Each vial was shaken for 45 s using a Vialmix® device (Lantheus Medical Imaging). Before introducing the ultrasound contrast agent in our setup, it was further diluted using a 0.9% saline solution.

The diluted ultrasound contrast agent was inserted using a syringe into a microbore tube with a 0.51-mm inner diameter. The tube led to a CUPROPHAN® RC55 cellulose capillary (Membrana GmbH, Wuppertal, Germany) with a 200-μm inner diameter and an 8-μm wall thickness. The middle of the capillary coincided with the optical focus of the objective lens and with the acoustic focus of the ultrasound transducer. The typical field of view using the 10 \times objective lens was 500 \times

$200(\mu\text{m})^2$, whereas the diameter of the acoustic focus was greater than 5 mm. Hence, the whole field of view could be considered in acoustic focus. The capillary was positioned 2 mm from the base of the container. The flow speed of the ultrasound contrast agent through the capillary was manually controlled.

RESULTS AND DISCUSSION

We observed the following stages of microfoam formation, illustrated in Figure 3. Our initial situation was a dense, random bubble distribution before ultrasound arrival. After the sonication started, contrast microbubbles collided, owing to secondary radiation forces. Subsequently, these clusters coalesced within the space of a quarter of the wavelength, owing to primary radiation forces. The resulting microfoams translated in the direction of the ultrasound field, owing to primary radiation forces.

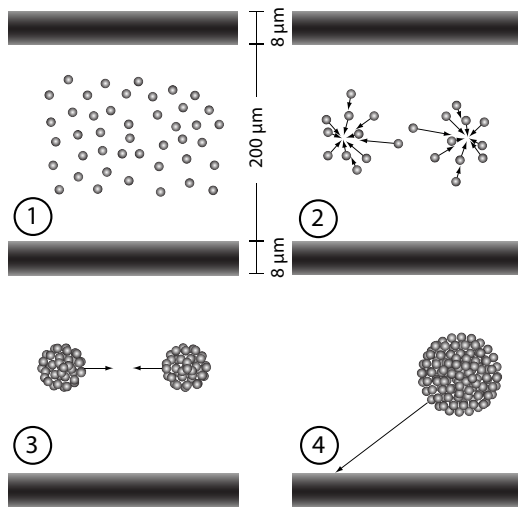


Figure 3: Schematic representation of the four stages of microfoam formation in a capillary: 1) random bubble distribution before ultrasound arrival; 2) bubbles colliding during sonication; 3) cluster coalescing within the space of a quarter of the wavelength; 4) microfoam translation.

With our bulk concentration, clusters were formed within seconds with diameters $25 \pm 2 \mu\text{m}$. The formation of clusters itself has been shown in more detail by Kotopoulos and Postema (2010). Taking into account the diameters of the microbubbles and their close packing in the cluster, we estimate that the clusters contain 2,000 microbubbles each. The clusters interact, owing to primary and secondary Bjerknes forces, creating morphing microfoams.

Figure 4 shows four interacting clusters in steady liquid. Primary Bjerknes forces pushed the clusters in the direction of the sound field at an average speed of 4 mm s^{-1} . The shear of the capillary wall caused a rotation of the interacting clusters, indicated by the arrows. Although exchange of individual bubbles between clusters took place, and pinch-off of small groups of bubbles was observed, the clusters as entities stuck together. The clusters had oval shapes, which can be attributed to secondary Bjerknes forces that increase exponentially at shorter distances to other bubble clusters.

Figure 5 shows at least eight interacting clusters. Again, a rotational motion can be observed. Also, individual ultrasound contrast agent microbubbles can be seen to hop from cluster to cluster. We attribute this behaviour on a microscopic scale to very subtle changes in the acoustic field, causing ever-changing local nodes and antinodes.

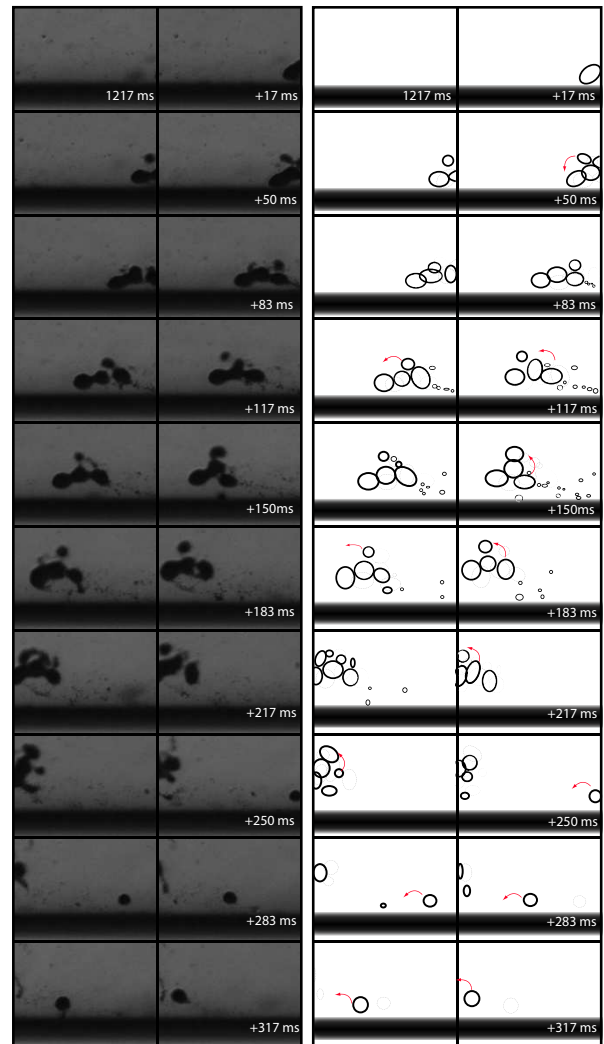


Figure 4: Morphing microfoam during sonication at 7 MHz and 86 kPa peak-negative pressure, and a schematic representation of the event. The frame size corresponds to $274 \times 198 (\mu\text{m})^2$. Time $t = 0$ was defined by the start of the sonication.

CONCLUSIONS

We have demonstrated that as soon as the bubble clusters are formed and as long as they are in the sound field, they behave as one entity. At our acoustic settings, it takes seconds to force the bubble clusters to positions approximately a quarter wavelength apart. The clusters contain approximately 2,000 ultrasound contrast agent microbubbles. Clusters streaming through a capillary interact, forming morphing microfoam.

Subjecting an ultrasound contrast agent of given concentration to a continuous low-amplitude signal makes it cluster to a microfoam of known position and known size, allowing for sonic manipulation, including the release of its contents. Alternatively, the microfoam could be removed from the blood pool, possibly using ultrasonics. The latter technique might be applicable in highly toxic ultrasound-guided drug delivery.

ACKNOWLEDGEMENTS

The authors are grateful to Lantheus Medical Imaging, North Billerica, MA, USA, for supplying the ultrasound contrast agent DEFINITY®. This work has been supported by DFG Emmy-Noether Programme grant 38355133, EPSRC grant EP/F037025/1 and the HERI Research Pump Priming Fund.

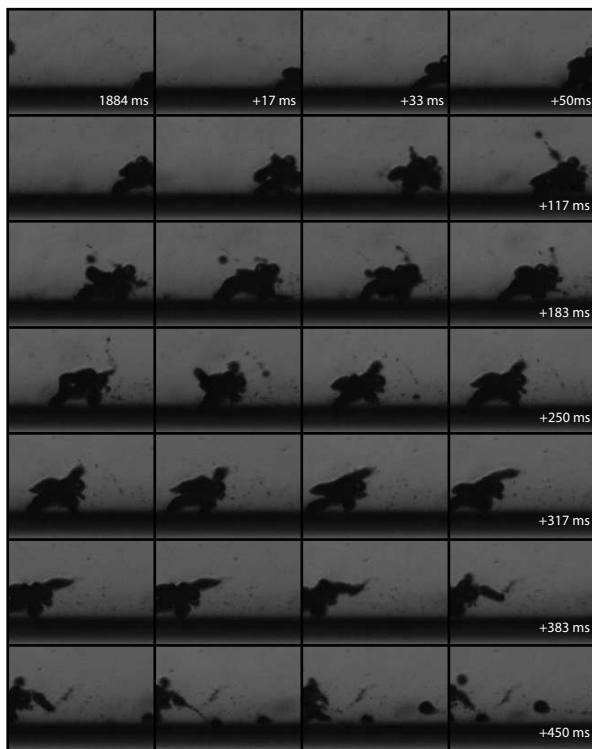


Figure 5: Morphing microfoam during sonication at 7 MHz and 86 kPa peak-negative pressure. The frame size corresponds to $274 \times 198 (\mu\text{m})^2$. Time $t = 0$ was defined by the start of the sonication.

REFERENCES

- P. A. Dayton, J. S. Allen, and K. W. Ferrara. The magnitude of radiation force on ultrasound contrast agents. *J. Acoust. Soc. Am.*, 112(5):2183–2192, 2002.
- E. Kimmel, B. Krasovitski, A. Hoogi, D. Razansky, and D. Adam. Subharmonic response of encapsulated microbubbles: condition for existence and amplification. *Ultrason. Med. Biol.*, 33(11):1767–1776, 2007.
- S. Kotopoulis and M. Postema. Microfoam formation in a capillary. *Ultrasonics*, 50(2):260–268, 2010.
- S. Kotopoulis, A. Schommartz, and M. Postema. Sonic cracking of blue-green algae. *Appl. Acoust.*, 70(10):1306–1312, 2009.
- N. Kudo, T. Miyaoka, K. Okada, K. Yamamoto, and K. Niwa. Study on mechanism of cell damage caused by microbubbles exposed to ultrasound. *Proc. IEEE Ultrason. Symp.*, pages 1351–1354, 2002.
- T. G. Leighton. *The Acoustic Bubble*. Academic Press Ltd, London, 1994.
- J. R. Lindner and S. Kaul. Delivery of drugs with ultrasound. *Echocardiography*, 18(4):329–337, 2001.
- H. Medwin. Counting bubbles acoustically: a review. *Ultrasonics*, 15:7–13, 1977.
- M. Postema and O. H. Gilja. Ultrasound-directed drug delivery. *Curr. Pharm. Biotechnol.*, 8(6):355–361, 2007.
- M. Postema, M. Mleczko, and G. Schmitz. Mutual attraction of oscillating microbubbles. In T. M. Buzug, D. Holz, S. Weber, J. Bongartz, M. Kohl-Bareis, and U. Hartmann, editors, *Advances in Medical Engineering*, volume 19 of *Methods of experimental physics*, pages 75–80. Springer, Berlin, 2007.
- M. Postema and G. Schmitz. Bubble dynamics involved in ultrasonic imaging. *Expert Rev. Mol. Diagn.*, 6(3):493–502, 2006.
- M. Postema and G. Schmitz. Ultrasonic bubble in medicine:

influence of the shell. *Ultrason. Sonochem.*, 14(4):438–444, 2007.

- P. Tortoli, E. Boni, M. Corsi, M. Ardit, and P. Frinking. Different effects of microbubble destruction and translation in Doppler measurements. *IEEE Trans. Ultrason., Ferroelect., Freq. Contr.*, 52(7):1183–1188, 2005.
- E. C. Unger, T. O. Matsunaga, T. McCreery, P. Schumann, R. Sweitzer, and R. Quigley. Therapeutic applications of microbubbles. *Eur. J. Radiol.*, 42:160–168, 2002.